Hexagonally Warped Dirac Cones and Topological Phase Transition in Silicene Superstructure

Motohiko Ezawa
Department of Applied Physics, University of Tokyo, Hongo 7-3-1, 113-8656, Japan

Silicene is a monolayer of silicon atoms forming a two-dimensional honeycomb lattice. We investigate electronic properties of the (4×4) superstructure, which is formed on top of the Ag(111) substrate. The band structure is obtained by folding that of silicene according to the superstructure. It is a peculiar feature that the two inequivalent K and K' points in the silicene Brillouin zone are identified by the folding. Consequently, two Dirac cones coexist at the same Dirac point in the momentum space. They are hexagonally warped by the Coulomb interaction. The silicene superstructure is a quantum spin-Hall insulator. It is surprising that the band gap never closes even if we apply the electric field. It is highly contrasted to the case of free-standing silicene, where a topological phase transition occurs. We then study generic superstructure and derive the conditions when the K and K' points are identified and when a topological phase transition may occur.

arXiv:1209.2580v1 [cond-mat.mes-hall] 12 Sep 2012

Graphene has attracted tremendous attention. Silicene is a sheet of silicon atoms replacing carbons in graphene. It could follow this trend[1–12] and open new perspectives for applications, especially due to its compatibility with Si-based electronics. Almost every striking property of graphene could be transferred to this innovative material. Indeed, it has Dirac cones akin to graphene. It has additionally a salient feature, that is a relatively large spin-orbit (SO) gap[6], which provides a mass to Dirac electrons and realizes a detectable quantum spin Hall (QSH) effect[7, 9]. Furthermore a topological phase transition occurs from the QSH insulator to the trivial band insulator in the electric field[9]. However, these properties are those of free-standing silicene. Silicene has been synthesized on metal surfaces that interact weakly with the silicon atoms[1–3].

Silicene available now is mostly grown on the Ag(111) substrate. The most often observed one is the so-called (4×4) superstructure[1, 2], though many other superstructures are possible due to the commensurability with the Ag substrate[13, 14]. Note that the symbol (4×4) refers to the structure of the Ag substrate. Indeed, there are 3×3 silicon atoms on top of 4×4 silver atoms in this structure. We should call it the (4×4) Ag-superstructure or the (3×3) Si-superstructure. The unit cell contains $2 \times (3 \times 3) = 18$ silicon atoms. The superstructure contain two sublattices: There are 6 (12) atoms in the higher (lower) sublattice which is 3.0Å (2.2Å) above the Ag surface, as illustrated in Fig.1. This structure has been observed in scanning tunneling microscopy (STM) images, where only the atoms in the higher sublattice are visible[1, 2].

In silicene the states near the Fermi energy are π orbitals residing near the inequivalent K and K' points at opposite corners of the hexagonal Brillouin zone. We refer to them also as the K$_\eta$ point with the valley index $\eta = \pm 1$. It is folded into a reduced Brillouin zone in a superstructure. Hence we can generally argue that the low-energy theory is described by massive Dirac electrons and that a silicene superstructure is a QSH insulator. However it is a nontrivial problem whether there exists a topological phase transition in the external electric field[9]. Furthermore, we may expect an intriguing phenomenon where the K and K' points are identified by the folding. When it happens, there exists only one Dirac point where two Dirac cones coexist, and this is experimentally detectable.

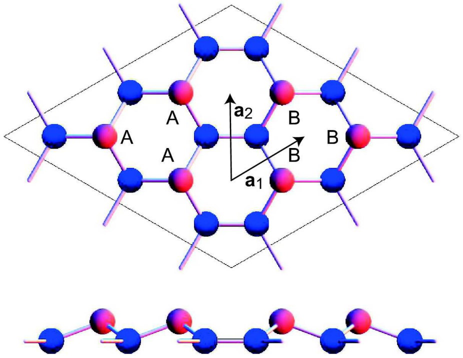

FIG. 1: (Color online) Unit cell of the (3×3) Si-superstructure. There are 18 silicon atoms per unit cell, in which 6 atoms are in higher position and 12 atoms are in lower position. There are 3 A and 3 B sites in higher position. Their vertical sepation is $2\ell \approx 0.8$Å.. The basis vectors are represented by $\boldsymbol{a}_i$.

In this paper we investigate electronic properties of the (3×3) Si-superstructure in detail. We show that the K and K' points are identified and that the band structure exhibits hexagonal warping in the presence of the Coulomb interaction. We also show that the band gap never closes even if we apply the electric field. We also make a discussion on generic silicene superstructure if the K and K' points are identified and if a topological phase transition occurs.

The (3×3) Si-superstructure system is described by the 36-band second-nearest-neighbor tight-binding model constructed as follows. The basic term is[15]

$$H_0 = -t \sum_{\langle i,j\rangle \alpha} c^\dagger_{i\alpha} c_{j\alpha} + i \frac{\lambda_{\rm SO}}{3\sqrt{3}} \sum_{\langle\langle i,j\rangle\rangle \alpha\beta} \nu_{ij} c^\dagger_{i\alpha} \sigma^z_{\alpha\beta} c_{j\beta}, \qquad (1)$$

where $c^\dagger_{i\alpha}$ creates an electron with spin polarization α at site i, and $\langle i,j\rangle$ / $\langle\langle i,j\rangle\rangle$ run over all the nearest/next-nearest neighbor hopping sites. The first term represents the usual nearest-neighbor hopping with the transfer energy $t = 1.6$eV.

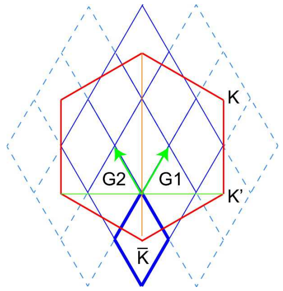

FIG. 2: (Color online) Brillouin zone of the (3×3) Si-superstructure. Its shape is rhombus. It is constructed by folding the Brillouin zone of silicene. The K and K' points are identified, which we denote by $\bar{\mathrm{K}}$ and take at the center of the Brillouin zone. The band structure along the horizontal and vertical thin lines are shown in Fig.3.

The second term represents the intrinsic SO coupling with $\lambda_{\mathrm{SO}} = 3.9$meV, where $\boldsymbol{\sigma} = (\sigma_x, \sigma_y, \sigma_z)$ is the Pauli matrix of spin, $\nu_{ij} = (\boldsymbol{d}_i \times \boldsymbol{d}_j) / |\boldsymbol{d}_i \times \boldsymbol{d}_j|$ with $\boldsymbol{d}_i$ and $\boldsymbol{d}_j$ the two bonds connecting the next-nearest neighbors. Additionally there exist two types of Rashba SO couplings (λ_{R1} and λ_{R2}) to describe silicene[10]. They are quite small, and play no important roles in the present analysis, as far as we have numerically checked. To avoid unnecessary complications, we neglect them.

The key feature of the (3×3) Si-superstructure is that it is made of higher and lower sublattices, which contain 6 and 12 silicon atoms per unit cell [Fig.1]. Each silicon atom is weakly bound to the silver substrate. The effect is summarized as a chemical potential difference U between silicon atoms in higher and lower sublattices. Additionally we may apply the electric field E_z perpendicular to the plane. It generates a staggered sublattice potential $\propto 2\ell E_z$ between them. The effective Hamiltonian is

$$H_1 = (U + 2\ell E_z) \sum_{i \in \mathrm{high}} c_i^\dagger c_i, \tag{2}$$

where the summation is taken over higher sites: U is a constant of the order of 0.1eV, and $2\ell \approx 0.8$Å according to the first-principle calculation[13].

The total Hamiltonian is $H = H_0 + H_1$, where the spin s_z is a good quantum number. Hence, the Hamiltonian is decomposed into the spin sectors indexed by $s_z = \pm 1$. It is enough to analyze the 18-band tight-binding model. We set $E_z = 0$ unless otherwise stated.

The Brillouin zone of a superstructure is constructed from that of silicene by identifying two momentum vectors $\boldsymbol{k}$ and $\boldsymbol{k}'$ provided they are different only by the principal reciprocal vectors $\boldsymbol{G}_1$ and $\boldsymbol{G}_2$, as illustrated in Fig.2. See (12) for the explicit form of $\boldsymbol{G}_i$. The band structure satisfies

$$\varepsilon(\boldsymbol{k} + \boldsymbol{G}_i) = \varepsilon(\boldsymbol{k}). \tag{3}$$

Accordingly the band structure is simply constructed by folding that of silicene when $U = 0$.

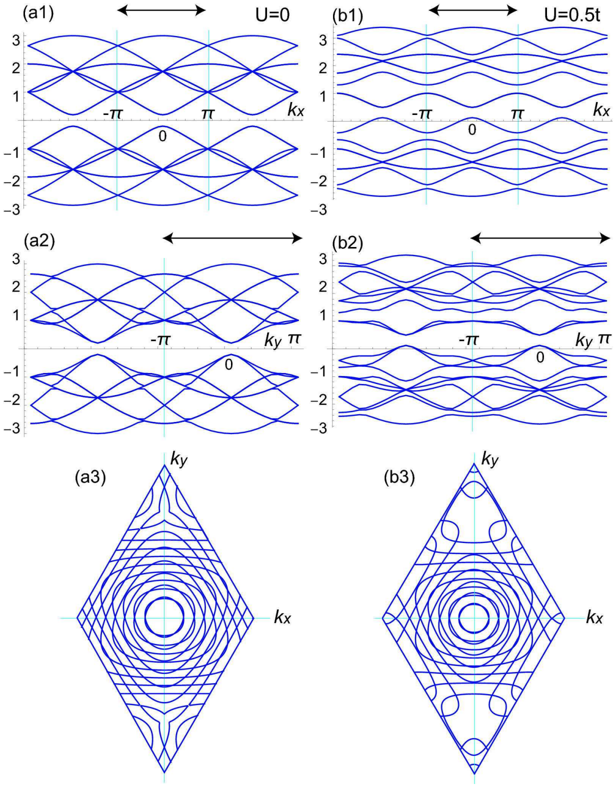

FIG. 3: (Color online) Band structure of the (3×3) Si-superstructure in extended Brillouin zone (a1,b1) along the k_x-axis and (a2,b2) along the k_y-axis. The vertical axis is the energy in unit of t. The horizontal axis is momentum k. (a3,b3) Contour plot of two trigonally warped Dirac cones. We have taken $U = 0$ for (a1,a2,a3) and $U = 0.5t$ for (b1,b2,b3). We have set $\lambda_{\mathrm{SO}} = 0.2t$ for illustration.

There may occur an intriguing phenomenon. In general, when there are two integers n_i such that

$$\boldsymbol{K} - \boldsymbol{K}' = n_1 \boldsymbol{G}_1 + n_2 \boldsymbol{G}_2, \tag{4}$$

the K and K' points are identified. We call it the $\bar{\mathrm{K}}$ point, and choose $\bar{\boldsymbol{K}} = (0, 0)$. Two Dirac cones coexist at the $\bar{\mathrm{K}}$ point.

This happens indeed in the (3×3) Si-superstructure, where the Brillouin zone is obtained by folding that of silicene two times along the k_x-axis and three times along the k_y-axis. The area of the Brillouin zone is $1/9$ of that of silicene, and its shape is rhombus. We show numerically calculated band structures of the superstructure for $U = 0$ and $U \neq 0$ in Fig.3, where we also show the contour plot of the band structures. There are two trigonally warped Dirac cones at the center of the Brillouin zone [Fig.3(a3,b3)].

These two Dirac cones cross each other. The level crossing will be transformed into the level anticrossing when Dirac electrons interact among themselves. We show the contour plots of the Dirac cones calculated based on the tight-binding model in Fig.4, where we have introduced an infinitesimal on-site Coulomb interaction. The two Dirac cones are now hexagonally warped, as must be experimentally detectable.

To understand this phenomenon analytically, we analyze

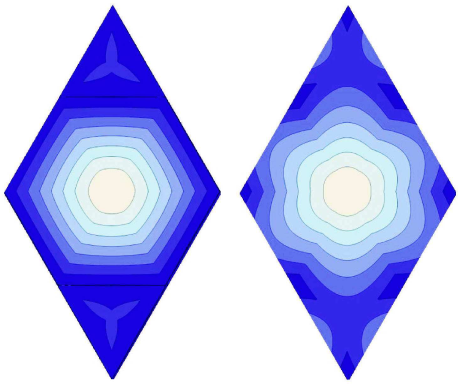

FIG. 4: (Color online) Contour plots of two hexagonally warped Dirac cones calculated based on the tight-binding model. They emerge when two crossing levels are transformed into two anticrossing levels by an infinitesimal on-site Coulomb interaction in trigonally warped Dirac dones in Fig.3(a3). We have taken $U = 0$ for simplicity. The Dirac cones are modified only slightly when $U \neq 0$.

the low energy Dirac theory of the Hamiltonian (1),

$$\begin{aligned} H_\eta &= \hbar v_{\text{F}} \left(k_x \tau_x + \eta k_y \tau_y \right) + \frac{\eta a e^{3\pi\eta i/2}}{4\sqrt{3}} \left(k_\eta^2 \sigma_+ + k_{-\eta}^2 \sigma_- \right) \\ & -\lambda_{\text{SO}} \sigma_z \eta \tau_z , \end{aligned} \tag{5}$$

where $\boldsymbol{\tau} = (\tau_x, \tau_y, \tau_z)$ is the Pauli matrix of pseudospin associated with the A and B sites. Two Dirac cones are labelled by η. The way of trigonal warping is represented by the factor $e^{3\pi\eta i/2}$ with the phase being opposite ($\eta = \pm 1$) between the two types of electrons[16]. Note that we cannot incorporate the potential term (2) into this simple Dirac theory. Hence we assume $U = 0$ in the analytical treatment.

When we introduce the on-site Coulomb interaction, the Hamiltonian H_{K} and $H_{\text{K'}}$ are mixed into

$$H = \begin{pmatrix} H_{\text{K}} & H_{12} \\ H_{21} & H_{\text{K'}} \end{pmatrix}, \tag{6}$$

where we have chosen the basis $\{c_A^K, c_B^K, c_A^{K'}, c_B^{K'}\}$, and

$$H_{\text{K}} = \begin{pmatrix} -\lambda_{\text{SO}} & \hbar v_{\text{F}} k_- + a e^{3\pi i/2} k_+^2 \\ \hbar v_{\text{F}} k_+ + a e^{-3\pi i/2} k_-^2 & \lambda_{\text{SO}} \end{pmatrix}, \tag{7}$$

$$H_{\text{K'}} = \begin{pmatrix} \lambda_{\text{SO}} & \hbar v_{\text{F}} k_+ - a e^{-3\pi i/2} k_-^2 \\ \hbar v_{\text{F}} k_- - a e^{3\pi i/2} k_+^2 & -\lambda_{\text{SO}} \end{pmatrix}. \tag{8}$$

$$H_{12} = H_{21} = \begin{pmatrix} V & 0 \\ 0 & V \end{pmatrix}, \tag{9}$$

with V representing the Coulomb energy. Up to the first order in V, the two bands are explicitly given by

$$\varepsilon_\pm^2 = (\hbar v_{\text{F}} k)^2 + \lambda_{\text{SO}}^2 + a^2 \pm \sqrt{2} a \hbar v_{\text{F}} k \sqrt{1 + \cos 6\theta}, \tag{10}$$

where θ is the azimuthal angle in the momentum space, $k_x = k \cos\theta$. We can check that these two band structures reproduce the hexagonally warped Dirac cones in Fig.4 quite well.

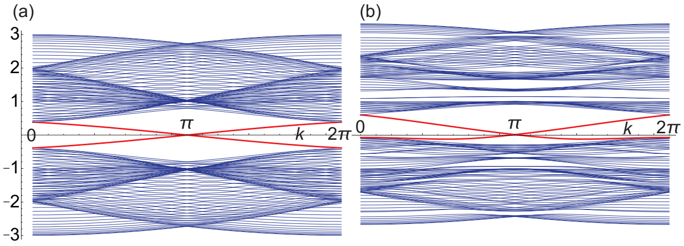

FIG. 5: (Color online) Band structure of nanorbibbon made of silicene superstructure. The vertical axis is the energy in unit of t. The horizontal axis is the momentum k. Two points $k = 0$ and $k = 2\pi$ are identified, and gives the $\bar{\text{K}}$ point. (a) $U = 0$. (b) $U = 0.5t$. We have set $\lambda_{\text{SO}} = 0.2t$ for illustration. Two lines connect the $\bar{\text{K}}$ point in the conduction and valence bands after winding once a circle of the whole Brillouin zone.

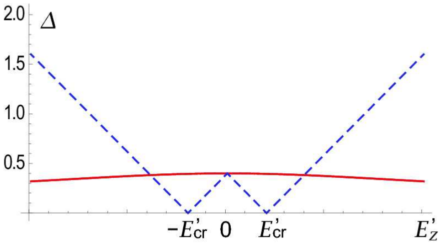

FIG. 6: (Color online) Band gap Δ as a function of the electric field $E_z' = E_z + U/2\ell$. We show Δ for the (3×3) Si-superstructure in the solid curves and for free-standing silicene in the dashed lines. The band gap closes at $E_{\text{cr}}' = \lambda_{\text{SO}}/\ell + U$ for the free-standing silicene. The vertical axis is the energy in unit of t. We have set $\lambda_{\text{SO}} = 0.2t$ for illustration.

The silicene superstructure is an insulator. In order to show that it is a QSH insulator, we have numerically calculated the band structure of a nanoribbon geometry in Fig.5. Two zero-energy edge modes are clearly seen: Each line represents the two-fold degenerate helical modes propagating one edge. It implies that the silicene superstructure is a QSH insulator. The band structure of a nanoribbon with $U = 0$ is just the one obtained by folding that of a silicene nanoribbon as in Fig.5(a). It is modified for $U \neq 0$, but the modification is only slight even when we take a quite large value for U, as shown in Fig.5(b). The essential feature is that the edge state connects the conduction and valence bands at the same $\bar{\text{K}}$ point. Nevertheless, the edge state is topologically protected since it winds a circle of the whole Brillouin zone as in Fig.5.

We now switch on the external electric field E_z in (2), and discuss the silicene superstructure in its presence. We show the band gap as a function of E_z in Fig.6. The band gap is found to be almost insensitive to E_z. It is surprising that the band gap never closes. This is highly contrasted to the case of free-standing silicene, where the band gap closes and a topological phase transition occurs[9] at a certain critical field E_{cr}. See (17) for discussions on this point.

We have studied the (3×3) Si-superstructure in detail. We proceed to make a discussion on generic silicene superstructure. All possible silicene superstructures are classified by the translational vectors $\boldsymbol{g}_1$ and $\boldsymbol{g}_2$ of the unit cell defined by

$$\boldsymbol{g}_1 = p\boldsymbol{a}_1 + q\boldsymbol{a}_2, \qquad \boldsymbol{g}_2 = e^{\pm i\pi/3}\boldsymbol{g}_1, \tag{11}$$

with the use of the two basis vectors $\boldsymbol{a}_1$ and $\boldsymbol{a}_2$ of the honeycomb lattice [Fig.1], and $0 \leq q \leq p$. The choice of the angle $\pm\pi/3$ generate a superstructure of type-I and type-II, respectively. When $q = 0$, type-I and type-II become identical. The reciprocal vectors $\boldsymbol{G}_1$ and $\boldsymbol{G}_2$ are

$$\boldsymbol{G}_i = (\boldsymbol{g}_i \times \boldsymbol{n})/\left|\boldsymbol{g}_1 \times \boldsymbol{g}_2\right|, \tag{12}$$

where $\boldsymbol{n}$ is the unit vector perpendicular to the silicene plane. By a geometrical analysis of the honeycomb lattice we have

$$|\boldsymbol{g}_1| = \sqrt{p^2 + q^2 + pq}. \tag{13}$$

The structure thus generated is the ($|\boldsymbol{g}_1| \times |\boldsymbol{g}_1|$) Si-superstructure. The number of silicon atoms per unit cell is given by

$$N = 2\left|\boldsymbol{g}_1\right|^2 = 2\left(p^2 + q^2 + pq\right). \tag{14}$$

The angle ϕ of the unit cell from the x-axis is given by

$$\tan\phi = \sqrt{3}q/(2p + q). \tag{15}$$

It is another problem on which Ag-superstructure this Si-superstructure is grown. Here we give some correspondences between them[13, 14]:

Ag-superstructure	Si-superstructure	p	q	ratio
4×4[1, 2]	3×3	3	0	1.33
$\sqrt{7} \times \sqrt{7}$	2×2	2	0	1.32
$\sqrt{13} \times \sqrt{13}$[2]	$\sqrt{7} \times \sqrt{7}$	2	1	1.36
$\sqrt{21} \times \sqrt{21}$	$2\sqrt{3} \times 2\sqrt{3}$	2	2	1.32
$2\sqrt{3} \times 2\sqrt{3}$[14]	$\sqrt{7} \times \sqrt{7}$	2	1	1.31

(16)

The ratios of the Ag and Si superstructures is around 1.3.

We have found that there exists no topological phase transition in the (3×3) Si-superstructure. It is important to explore the same problem in generic superstructure. We assume that the buckled structure consists of two sublattices. Indeed, there is a report[13] that this is the case for all structures grown on Ag(1,1,1). Let the numbers of A sites and B sites be N_A and N_B, respectively, in the higher sublattice per unit cell which contains N silicon atoms. As we have stated, we cannot incorporate the potential term (2) into the simple Dirac theory (5). Nevertheless, it can be argued to yield a contribution to the Dirac mass m_D within the mean-field approximation,

$$m_D = \frac{N_A - N_B}{N}(U + 2\ell E_z) + \eta s_z \lambda_{\text{SO}}. \tag{17}$$

The phase transition would occur [11] at $m_D = 0$, which determines the critical field E_{cr}. In the case of free-standing silicene, we have $U = 0$, $N_A = 1$, $N_B = 0$, $N = 2$, and hence

$$E_{\text{cr}} = \lambda_{\text{SO}}/\ell, \tag{18}$$

as agrees with the previous result[9]. In the present (3×3) Si-superstructure, we have $N_A = N_B = 3$, $N = 18$, and we find $E_{\text{cr}} \to \infty$, or equivalently there is no phase transition point.

In conclusion, we have investigated the (3×3) buckled superstructure of silicene. It is found that the K and K' points become identical and hence two Dirac cones coexist at the $\bar{\text{K}}$ point. They exhibit hexagonal warping in the presence of the Coulomb interaction, which must be observed by angle resolved photoemission spectroscopy (ARPES). It is also found that there is no topological phase transition. Furthermore we have explored electronic properties of generic superstructure. The K and K' points become identified when the condition (4) is satisfied. We may expect a topological phase transition when the numbers of the A and B sites are different in the higher sublattice of the backed silicene superstructure.

I am very much grateful to G.L. Lay, S. Hasegawa and N. Nagaosa for many fruitful discussions on the subject. This work was supported in part by Grants-in-Aid for Scientific Research from the Ministry of Education, Science, Sports and Culture No. 22740196.

[1] P. Vogt, , P. De Padova, C. Quaresima, J. A., E. Frantzeskakis, M. C. Asensio, A. Resta, B. Ealet and G. L. Lay, Phys. Rev. Lett. **108**, 155501 (2012).

[2] C.-L. Lin, R. Arafune, K. Kawahara, N. Tsukahara, E. Minamitani, Y. Kim, N. Takagi, M. Kawai, Appl. Phys. Express 5, Art No. 045802 (2012) .

[3] A. Fleurence, R. Friedlein, T. Ozaki, H. Kawai, Y. Wang, and Y. Yamada-Takamura, Phys. Rev. Lett. **108**, 245501 (2012).

[4] K. Takeda and K. Shiraishi, Phys. Rev. B **50** 075131 (1994).

[5] Gian G. Guzmán-Verri and L. C. Lew Yan Voon, Phys. Rev. B **76** 075131 (2007).

[6] S. Cahangirov, M. Topsakal, E. Aktürk,1 H. Sahin, and S. Ciraci, Phys. Rev. Lett. **102**, 236804 (2009).

[7] C.-C. Liu, W. Feng, and Y. Yao, Phys. Rev. Lett. **107**, 076802 (2011).

[8] C.-C. Liu, H. Jiang, and Y. Yao, Phys. Rev. B, **84**, 195430 (2011).

[9] M. Ezawa, New J. Phys. **14**, 033003 (2012).

[10] M. Ezawa, Phys. Rev. Lett. **109**, 055502 (2012).

[11] M. Ezawa, cond-mat/arXiv:1205.6541 (to appear in Euro. Phys. J. B)

[12] M. Ezawa, J. Phys. Soc. Jpn. **81**, 064705 (2012): Europhysics Letters **98**, 67001 (2012): cond-mat/arXiv:1204.3971: cond-mat/arXiv:1206.5378: cond-mat/arXiv:1207.6694.

[13] H. Enriquez, S. Vizzini, A. Kara, B. Lalmi and H. Oughaddou, J. Phys.: Condens. Matter **24,** 24314211 (2012).

[14] H. Jamgotchian, Y. Colignon, N. Hamzaoui, B. Ealet, J. Y. Hoarau, B. Aufray and J P Biberian, J. Phys.: Condens. Matter **24,** 172001 (2012).

[15] C. L. Kane and E. J. Mele, Phys. Rev. Lett. **95**, 226801 (2005).

[16] H. Ajiki and T. Ando, J. Phys. Soc. Jpn. **65**, 505 (1996).